

Deep learning based photoplethysmography classification for peripheral arterial disease detection: a proof-of-concept study

Allen, J., Liu, H., Iqbal, S., Zheng, D. & Stansby, G.

Author post-print (accepted) deposited by Coventry University's Repository

Original citation & hyperlink:

Allen, J, Liu, H, Iqbal, S, Zheng, D & Stansby, G 2021, 'Deep learning based photoplethysmography classification for peripheral arterial disease detection: a proof-of-concept study', *Physiological Measurement*, vol. (In-Press), pp. (In-Press).
<https://dx.doi.org/10.1088/1361-6579/abf9f3>

DOI 10.1088/1361-6579/abf9f3

ISSN 0967-3334

ESSN 1361-6579

Publisher: IOP Publishing

As the Version of Record of this article is going to be / has been published on a gold open access basis under a CC BY 3.0 licence, this Accepted Manuscript is available for reuse under a CC BY 3.0 licence immediately.

This document is the author's post-print version, incorporating any revisions agreed during the peer-review process. Some differences between the published version and this version may remain and you are advised to consult the published version if you wish to cite from it.

ACCEPTED MANUSCRIPT • OPEN ACCESS

Deep learning based photoplethysmography classification for peripheral arterial disease detection: a proof-of-concept study

To cite this article before publication: John Allen *et al* 2021 *Physiol. Meas.* in press <https://doi.org/10.1088/1361-6579/abf9f3>

Manuscript version: Accepted Manuscript

Accepted Manuscript is “the version of the article accepted for publication including all changes made as a result of the peer review process, and which may also include the addition to the article by IOP Publishing of a header, an article ID, a cover sheet and/or an ‘Accepted Manuscript’ watermark, but excluding any other editing, typesetting or other changes made by IOP Publishing and/or its licensors”

This Accepted Manuscript is © 2021 Institute of Physics and Engineering in Medicine.

As the Version of Record of this article is going to be / has been published on a gold open access basis under a CC BY 3.0 licence, this Accepted Manuscript is available for reuse under a CC BY 3.0 licence immediately.

Everyone is permitted to use all or part of the original content in this article, provided that they adhere to all the terms of the licence <https://creativecommons.org/licenses/by/3.0>

Although reasonable endeavours have been taken to obtain all necessary permissions from third parties to include their copyrighted content within this article, their full citation and copyright line may not be present in this Accepted Manuscript version. Before using any content from this article, please refer to the Version of Record on IOPscience once published for full citation and copyright details, as permissions may be required. All third party content is fully copyright protected and is not published on a gold open access basis under a CC BY licence, unless that is specifically stated in the figure caption in the Version of Record.

View the [article online](#) for updates and enhancements.

1
2
3
4
5 1 **Deep learning based photoplethysmography**
6
7
8 2 **classification for peripheral arterial disease**
9
10
11 3 **detection: a proof-of-concept study**
12
13
14 4

15
16 5 **John Allen^{1,2,3}, Haipeng Liu², Sadaf Iqbal^{1,3}, Dingchang Zheng^{1,2}, Gerard Stansby⁴**
17
18
19 6

20
21 7 ¹Faculty of Medical Sciences, Newcastle University, Newcastle upon Tyne. UK.
22

23 8 ²Research Centre for Intelligent Healthcare, Coventry University. UK.
24

25
26 9 ³Northern Regional Medical Physics Department, Freeman Hospital, Newcastle
27
28 10 upon Tyne. UK.

29
30 11 ⁴Northern Vascular Centre, Freeman Hospital, Newcastle upon Tyne. UK.
31
32

33 12
34 13
35 14 Corresponding author (JA): John Allen (John.AllenVO@ieee.org)
36

37 15
38 16 Journal: **Physiological Measurement**
39

40 17
41 18 Manuscript version: 13th April 2021
42

43 19
44 20 Total number of words: ~3300 (Abstract <250)
45
46 21
47 22
48 23

49 24
50 25 Short running title: **Deep learning PPG detection of PAD**
51
52 26
53 27
54 28

55 29 **Keywords:** AI, Artery, Deep Learning, Peripheral Arterial Disease,
56 30 Photoplethysmography, Pulse, Wavelet
57
58 31
59
60

32 Abstract

33 **Objective:** A proof-of-concept study to assess the potential of a Deep Learning
34 (DL) based photoplethysmography PPG ('DLPPG') classification method to
35 detect peripheral arterial disease (PAD) using toe PPG signals.

36 **Approach:** PPG spectrogram images derived from our previously published
37 multi-site PPG datasets (214 participants; 31.3% legs with PAD by Ankle Brachial
38 Pressure Index (ABPI)) were input into a pretrained 8-layer (5 Convolutional
39 Layers + 3 Fully Connected Layers) AlexNet as tailored to the 2-class problem
40 with transfer learning to fine tune the Convolutional Neural Network (CNN). k-fold
41 random cross validation (CV) was performed [for k=5 and k=10], with each
42 evaluated over k training / validation runs. Overall test sensitivity, specificity,
43 accuracy, and Cohen's Kappa statistic with 95% confidence interval ranges were
44 calculated and compared, as well as sensitivities in detecting mild-moderate
45 ($0.5 \leq \text{ABPI} < 0.9$) and major ($\text{ABPI} < 0.5$) levels of PAD.

46 **Main results:** Cross validation with either k = 5 or 10 folds gave similar diagnostic
47 performances. The overall test sensitivity was 86.6%, specificity 90.2% and
48 accuracy 88.9% (Kappa: 0.76 [0.70-0.82]) (at k=5). The sensitivity to mild-
49 moderate disease was 83.0% (75.5-88.9%) and to major disease was 100.0%
50 (90.5-100.0%).

51 **Significance:** Substantial agreements have been demonstrated between the DL-
52 based PPG classification technique and the ABPI PAD diagnostic reference. This
53 novel automatic approach, requiring minimal pre-processing of the pulse
54 waveforms before PPG trace classification, could offer significant benefits for the
55 diagnosis of PAD in a variety of clinical settings where low-cost, portable and
56 easy-to-use diagnostics are desirable.

57

58

59

60

61

62 1. Introduction

63 Peripheral arterial disease (PAD) of the lower limbs is a common form of
64 widespread atherosclerosis and is associated with an increased risk of coronary
65 artery disease and stroke (Abdulhannan *et al.*, 2012). PAD prevalence increases
66 with age, especially in smokers and diabetics. Its diagnosis can be made on
67 clinical grounds, but other conditions such as musculoskeletal, spinal disease
68 and venous disease may also produce similar exercise induced symptoms. There
69 are a range of tests to assess patients for possible PAD and this includes the
70 widely used reference standard of an Ankle Brachial Pressure Index (ABPI) <0.9.
71 The operation of ABPI measurement, however, typically takes 10-30 minutes
72 even by specialist operators, may be inaccurate with vessel calcification and can
73 cause discomfort and pain in some patients (Scott *et al.*, 2019).

74 Ideally a vascular screening technology for PAD should be low-cost, quick,
75 reliable, repeatable, non-invasive, portable and simple to operate. One technique
76 that has this potential is the low-cost optical pulse wave technology:
77 photoplethysmography (PPG). PPG signals are derived from the changes in the
78 blood volume in the microvascular bed of tissue, therefore can reflect on the
79 properties of cardiovascular system in time and frequency domains (Allen, 2007).
80 PPG signals can be measured at many different body sites (Perpetuini *et al.*,
81 2019; Chan *et al.*, 2019) although the toe site has been popular for developing
82 methods to detect vascular disease. It is accepted that the peripheral PPG pulse
83 wave usually becomes damped, delayed and diminished with increasing severity
84 of PAD, which makes the PPG-based detection of PAD possible (Allen & Murray,
85 1993). In the recent works by our wider Newcastle research group, the PAD-

1
2
3
4 86 related changes in PPG waveform characteristics have been quantitatively
5
6 87 investigated in subjects in different age groups and for PPG 'AC' as well as its
7
8 88 lower frequency 'DC' components (Allen *et al.*, 2008; Allen *et al.*, 2005; Bentham
9
10 89 *et al.*, 2018). The results indicate the potential value of using just bilateral great
11
12 90 toe PPG measurements for low-cost and simple-to-do PAD detection. It has been
13
14 91 suggested that the pulse wave from the great toe pad might be a better body site
15
16 92 than ankle in detecting PAD, especially in "challenging populations" as those
17
18 93 exhibiting arterial calcification (Herraiz-Adillo *et al.*, 2020).
19
20 94 As a promising approach towards large-scale healthcare services, the analysis
21
22 95 of PPG signals based on deep learning (DL) has been recently applied to
23
24 96 cardiovascular field for the detection of heart rate (Reiss *et al.*, 2019),
25
26 97 hypertension (Liang *et al.*, 2018), arterial fibrillation (Cheng *et al.*, 2020). DL can
27
28 98 accurately detect multiple PAD-related cardiovascular risks (e.g., hypertension,
29
30 99 diabetes, cerebral infarction) (Panwar *et al.*, 2020). It has been suggested in two
31
32 100 recent studies that DL-based PPG analysis could be useful in the detection of
33
34 101 diseases of the arteries (Lee *et al.*, 2020; Panwar *et al.*, 2020). A DL-based
35
36 102 analysis of the second derivative of the finger PPG trace showed a high accuracy
37
38 103 in the prediction of the ABPI class for severity of arterial disease (accuracy
39
40 104 98.34%, for six ABPI classes covering mild through to severe disease, arterial
41
42 105 hardening, and normal) (Lee *et al.*, 2020), although there could have been
43
44 106 overtraining which compensated for known accuracy limitations with ABPI
45
46 107 reference for PAD. Since PAD symptoms can manifest themselves early in the
47
48 108 legs then it is considered appropriate to study the PPG measurements obtained
49
50 109 more directly from the lower limbs. However, as far as we know there is a clear
51
52 110 lack of DL-based studies on the detection of PAD based using PPG signals
53
54
55
56
57
58
59
60

1
2
3
4 111 collected from the toes. The aim of this proof-of-concept study was to assess the
5
6 112 potential of a DL-based method for automatically detecting the presence (or
7
8 113 absence) of PAD from the toe PPG measurements as well as its sensitivity to
9
10
11 114 detecting higher and lower grade disease.
12
13
14 115

16 116 **2. Methods**

18 117 **2.1 Measurements**

20
21 118 The physiological measurements are described in detail in (Allen *et al.*, 2005;
22
23 119 Allen *et al.*, 2008). In summary, they were performed in a warm temperature-
24
25 120 controlled room (24 ± 1 °C), and at least 10 minutes were given for thermal
26
27 121 acclimatization and relaxation. Measurements were made by a single operator
28
29 122 (JA) with subjects in the supine position, firstly with the ABPI measurements for
30
31 123 both legs as the 'gold standard' reference for the presence of PAD (i.e., <0.9,
32
33 124 using highest of the right and left ankle systolic blood pressures), and secondly
34
35 125 the bilateral PPG great toe pulse measurements from a multi-site PPG pulse
36
37 126 measurement concept prototype system. The PPG measurement system
38
39 127 simultaneously acquired bilateral toe pulses using electronically matched pairs of
40
41 128 right and left pulse amplifiers of bandwidth (0.15–20 Hz, single pole high pass
42
43 129 filtering) with data captured to computer for subsequent pulse wave analysis for
44
45 130 at least 2.5 minutes (Allen & Hedley, 2019). Subject age, gender and height were
46
47 131 also recorded.
48
49
50
51
52

53 132 54 55 133 **2.2 Subjects**

1
2
3
4 134 The two cohorts studied using the same protocol were combined to evaluate the
5
6 135 DL-based PAD classifier and these sets are summarized in our 2005 pilot
7
8 136 evaluation paper (Allen 2002, Allen *et al.*, 2005) and our 2008 prospective study
9
10
11 137 paper (Allen *et al.*, 2008). In summary, they comprised a mixture of older subjects,
12
13 138 with and without significant lower limb occlusive PAD. Subjects were excluded if
14
15 139 they had an obvious cardiac arrhythmia, lower limb amputation, vasculitis,
16
17 140 significant movement artefact (for example due to limb tremor), skin problems
18
19 141 (e.g., cuts or bruising at a measurement site or photosensitive skin) and
20
21 142 Raynaud's phenomenon. We did not specifically exclude those with hypertension,
22
23 143 diabetes, hypercholesterolaemia, chronic renal failure or ischaemic heart disease
24
25 144 as these are all relevant to the atherosclerotic phenotype. All subjects gave their
26
27 145 written informed consent. More recent further ethical approval was also granted
28
29 146 for a further re-analysis of the anonymized sets of PPG waveforms (Newcastle
30
31 147 University Ethics Committee, 7840/2020). The combined 2 studies gave a total of
32
33 148 218 potential subjects although a small number of these subjects (3) had elevated
34
35 149 ABPIs (>1.4 in either leg) which were excluded owing to the risk of false negative
36
37 150 results observed when ABPI is used in calcified blood vessels. A further subject
38
39 151 was excluded as they were found to show a consistent cardiac arrhythmia on their
40
41 152 pulse traces. In total therefore, PPG toe pulses from 214 subjects were available
42
43 153 for subsequent DL classification and study, comprising 134 subjects having
44
45 154 normal arteries in both legs and 80 subjects having significant vascular disease
46
47 155 in at least one leg (i.e., 37.4% of the total by subject; 31.3% of legs having PAD)
48
49 156 by ABPI classification.
50
51
52
53
54
55
56
57
58

59 158 **2.3 PPG Pulse analysis**

159 2.3.1 Signal pre-processing

160 The raw PPG signals for right and left great toes over 2.5 minutes were pre-
161 processed using detrending by removing their mean levels, and then normalizing
162 to unit variance. No pre-filtering or denoising stages were employed. A
163 continuous wavelet transform (CWT, 'amor' i.e., Gabor wavelet MATLAB,
164 MathWorks Inc., version 2020a) was applied and a spectrogram image produced
165 for each great toe measurement, i.e., for both right and left legs separately, and
166 covering the 2.5 minute period (\log_{10} y-axis: 0.0312 to 8 Hz to capture the
167 dynamics of the PPG signal over time, Figure 1). The intensity for the colour bar
168 of each CWT spectrogram was auto scaled, the image then saved in *.png file
169 format. This gave 428 files (by ABPI reference standard: 292 / 136 legs without /
170 with PAD, in which 94 legs with mild-moderate disease and 40 legs with major
171 disease) for subsequent DL training and cross validation testing.

173 2.3.2 Deep learning convolutional neural network and training

174 Convolutional Neural Network (CNN) is a class of DL networks that is designed
175 to learn features from the input data using its multiple Convolutional Layers. The
176 DL analysis was performed using MATLAB Deep Learning Toolbox software (The
177 Mathworks Inc., Natick, Massachusetts, United States) on a standard computing
178 platform. AlexNet (<http://alexlenail.me/NN-SVG/AlexNet.html>) was used which is
179 a pre-trained CNN that has been pre-trained on a database named ImageNet
180 consisting of more than 1.2 million images belonging to one thousand classes
181 (Krizhevsky *et al.*, 2012). AlexNet is well known (Krizhevsky *et al.*, 2012; Lu *et*
182 *al.*, 2019; Wang *et al.*, 2019). Briefly, its structure has 8 layers: five Convolutional
183 Layers (CL1 to 5) and three Fully Connected Layers (FCL6-8), with Rectified

1
2
3
4 184 Linear Unit (ReLU) as the activation function. The final FCL8 layer was tailored
5
6 185 to the 2-class problem (Figure 2) (Wang *et al.*, 2019). Transfer learning was
7
8 186 applied for fine tuning of specific layers of the CNN. Treating each leg separately,
9
10 187 each great toe PPG spectrogram image was rescaled to the AlexNet CNN input
11
12 188 layer structure size of 227x227 pixels, with 3-colour channels of red, green and
13
14 189 blue. The 2 CNN outputs gave the classification outcome of 'no PAD' and 'PAD'.
15
16 190 With the absence of fixed rules for deep learning parameter selection in the
17
18 191 literature then initial experiments were carried out within the Matlab Deep
19
20 192 Learning Toolbox development environment to set the key parameters for
21
22 193 AlexNet-based PAD / PPG application. The learning rate and the momentum
23
24 194 term parameters were initially and briefly explored in the ranges of 0.00001 to
25
26 195 0.01 and 0.4 to 0.9, respectively, with learning considered to be demonstrated
27
28 196 when there was a trajectory towards an acceptable classification performance
29
30 197 (e.g., 75-100%) at each fold tested (using 30 epochs with mini-batch size 20),
31
32 198 i.e., without the algorithm getting stuck at the low starting performance level. The
33
34 199 choice of number of epochs depends on training and validation error. Keeping
35
36 200 the number of epochs small can lead to underfitting while making this number
37
38 201 high can lead to overfitting of the model. In our study, the validation error
39
40 202 trajectory approached a minimum at 30 epochs and hence this number was
41
42 203 selected. Subsequently, a learning rate of 0.001 and momentum term of 0.5 were
43
44 204 selected for the k-fold cross validation testing as these showed learning across
45
46 205 all folds and carried out with reasonable speed. To aid the learning and
47
48 206 generalization then pixel shift and image augmentation were also incorporated
49
50 207 into the training stage.
51
52
53
54
55
56
57
58
59
60

209 2.3.3 Consistency with k-fold cross validation

210 As there is no standardization in the choice of k for k-fold random cross validation
211 we experimented with two different values (k=5 and k=10), with k training /
212 validation runs, as applied in existing studies on DL-based PPG signal analysis
213 (Dall'Olio *et al.*, 2020; He *et al.*, 2016). For each training run the image sets were
214 randomly split into a training set and a validation set, with transfer learning from
215 the PPG spectrogram images. At each training run the confusion matrix was
216 updated, and on the completion of all runs the overall test sensitivity, specificity
217 and accuracy (with 95% confidence interval ranges) were calculated. The
218 process was repeated for k set to 10 enabling a simple comparison of the
219 classification performance obtained for a k-fold value of 5.

220

221 2.3.5 Statistical analysis and diagnostic performance assessments

222 Clinical measurements were summarized using median and inter-quartile range
223 [IQR, 25th percentile to 75th percentile], calculated using simple Microsoft Office
224 Excel spreadsheet functions. Cross-tabulation of PAD status by ABPI and DL
225 classifier was performed from which associated diagnostic test accuracy (DTA)
226 measures of sensitivity, specificity, and diagnostic accuracy, were determined
227 alongside associated 95% confidence intervals overall, as well as per severity
228 classification. DTA statistical analyses were performed using SciStat.com online
229 statistical software © 2020 MedCalc Software Ltd. The sensitivities in detecting
230 overall disease (ABPI<0.9), mild-moderate disease ($0.5 \leq ABP < 0.9$) and major
231 disease (ABPI <0.5) were calculated for the PPG spectrogram image sets.
232 Cohen's Kappa statistic and 95% CI ranges were also calculated for the
233 diagnostic performances (McHugh, 2012) on SPSS (SPSS 21.0 for Windows,

1
2
3
4 234 SPSS Inc., Chicago, IL), noting a Kappa value between 0.41 and 0.6 represents
5
6 235 moderate agreement; between 0.61 and 0.8 represents substantial agreement;
7
8 236 and 0.81 and 1.00 represents almost perfect agreement.
9
10

11 237

13 238 **3. Results**

15 239 Toe PPG pulse spectrogram images from a total of 214 subjects (137 males, 77
16
17 240 females) were classified using deep learning. The median [IQR] age was 64 [52
18
19 241 - 72] years, systolic blood pressure 142 [128 - 160] mmHg, and height 1.69 [1.60
20
21 242 - 1.70] m.
22
23
24
25 243

26
27 244 The overall diagnostic performances with AlexNet DL classification are shown in
28
29 245 Tables 1 and 2, with all comparisons having substantial agreement (by Cohen's
30
31 246 Kappa statistic, i.e., for agreement beyond chance) with ABPI. The tables also
32
33 247 summarize the values (and 95% CI ranges) of sensitivity, specificity and accuracy
34
35 248 for k=5 (and 10) over the k repeat training / validation runs.
36
37
38

39 249 For k=5 the overall test sensitivity was 86.6 (95% CI: 80.6-91.3) %, specificity
40
41 250 90.2 (86.2-93.3) %, accuracy 88.9 (85.7-91.6) %, and Kappa 0.76 [0.70-0.82]).
42
43

44 251 The test sensitivity was clearly higher overall for the legs with higher grade PAD,
45
46 252 with 83.0 (75.5-88.9) % for mild-moderate disease vs 100.0 (90.5-100.0) % for
47
48 253 major disease, giving Cohen's Kappa values of 0.72 (0.65-0.79) and 0.67 (0.56-
49
50 254 0.78), respectively.
51
52

53 255 For k=10 the results were similar to the k=5 results, with overall test sensitivity
54
55 256 82.4 (95% CI: 74.8-88.5) %, specificity 89.0 (84.8-92.3) % and accuracy 86.9
56
57 257 (83.3-90.0) %, and Kappa 0.70 [0.63-0.77]). As with k=5, the test sensitivity was
58
59
60

1
2
3
4 258 clearly higher overall for the legs with higher grade PAD, with 77.3 (67.7-85.2) %
5
6 259 for mild-moderate disease vs 97.1 (84.7-99.9) % for major disease, giving
7
8 260 Cohen's Kappa values of 0.64 (0.55-0.73) and 0.61 (0.50-0.73), respectively.
9
10

11 261

12 262 **4. Discussion**

13
14 263 An innovative DL-based PPG Classifier ('DLPPG') approach using pre-trained
15
16 264 Convolutional Neural Network AlexNet with fine tuning by transfer learning to
17
18 265 diagnose PAD from toe PPG measurements has been evaluated in this study,
19
20 266 with performance assessed in this proof-of-concept study to show substantial
21
22 267 agreements overall with the ABPI vascular reference for PAD.
23
24
25

26
27
28 268 Currently, PAD diagnostics depends on mainly on ABPI measurement as the
29
30 269 first-line test. In the 2016 American Heart Association (AHA) / American College
31
32 270 of Cardiology (ACC) Guideline on PAD, the technological advancement for
33
34 271 simplified diagnosis of PAD and critical limb ischemia is listed as a major research
35
36 272 direction (Gerhard-Herman *et al.*, 2017). The proposed DL-based analysis of the
37
38 273 toe PPG signal provides the possibility for quick assessment and follow-up over
39
40 274 time, and low-cost management of PAD. The novel DL-based approach
41
42 275 assessed in this study has advantages over previously reported approaches
43
44 276 (e.g., analysis involving fiducial waveform characteristics) (Karimian *et al.*, 2017)
45
46 277 in PPG pulse analysis, with some earlier methods (Allen 2000; Allen *et al.*, 2005;
47
48 278 Allen *et al.*, 2008) being resource intensive in pre-processing as they required the
49
50 279 manual checking by an expert operator on a beat by beat basis to mark and
51
52 280 exclude noisy pulses, and noting that derived pulse timing features and
53
54 281 normalised pulse shapes are dependent on digital filter types which can be
55
56
57
58
59
60

1
2
3
4 282 difficult to replicate for devices working on-line i.e., in real time. In contrast, this
5
6 283 new approach based on deep learning required minimal data pre-processing and
7
8 284 had no denoising stage.
9

10
11 285 The manual extraction of physiological parameters from time-frequency spectra
12
13 286 is cumbersome, highly parametrised, and tailored to specific scenarios, whereas
14
15 287 the DL-based PPG analysis is appropriate for the large-scale application on
16
17 288 bespoke measurement devices (Wilkes *et al.* 2015; Reiss *et al.*, 2019) as well as
18
19 289 centralised cloud-based signal diagnostics. Ultimately, such pulse assessments
20
21 290 could improve the management of patients with PAD by giving accessible and
22
23 291 timely feedback to the patient and their doctors to help them reduce their
24
25 292 associated risk factors for cardiovascular disease.
26
27
28

29
30 293 The AHA/ACC Guideline also highlighted the need for the improvement of clinical
31
32 294 classification systems for PAD that incorporate symptoms, anatomic factors, and
33
34 295 patient-specific risk factors and can be used to predict clinical outcome and
35
36 296 optimize treatment approach (Gerhard-Herman *et al.*, 2017). Our results showed
37
38 297 substantial accuracy, sensitivity, and Cohen's Kappa values for legs with mild-
39
40 298 moderate PAD as well as for major PAD, although the detection sensitivity was
41
42 299 lower for lower grade disease. These classification performances appear similar
43
44 300 to the results of our earlier studies based on specific characteristics of the PPG
45
46 301 toe pulse, e.g., using careful manual extraction of normalised shape, risetime and
47
48 302 amplitude features (Allen *et. al.* 2005; Allen *et. al.* 2008) for overall accuracy and
49
50 303 differences with PAD severity in the legs. Our new approach also includes
51
52 304 information on the dynamics of the PPG, i.e., the 'DC' lower frequency
53
54 305 components, in health and disease and this could well yield additional important
55
56
57
58
59
60

1
2
3
4 306 information that aids the diagnosis and understanding of the disease process, for
5
6 307 example for diabetic patients with PAD where there is autonomic involvement
7
8 308 and/or vascular calcification, and this should be further explored as an exciting
9
10
11 309 way forward in vascular assessment.

12
13
14 310 Other research groups have explored the use of DL-based PPG analysis in
15
16 311 vascular assessments, including Lee *et al.* (2020) who used a convolutional long
17
18 312 short term memory model (C-LSTM: with 5 convolutional layers, 5 pooling layers
19
20 313 and one LSTM layer) to classify the second derivative of the finger PPG trace to
21
22 314 predict the ABPI class i.e., severity of arterial disease (data from MIMIC-III
23
24 315 database, Johnson *et al.*, 2006). Their results are impressive and in
25
26 316 approximately 1000 subjects attained an accuracy of greater than 98% (for six
27
28 317 ABPI classes covering mild through to severe disease, arterial hardening, and
29
30 318 normal). They did combine 2 DL models (CNN and LSTM) which could have
31
32 319 improved performance, compared to the results from our single DL model.
33
34 320 However, there may be an element of over-fitting which somehow compensates
35
36 321 for the imperfect ABPI reference for PAD. Such results do show what can be
37
38 322 possible with deep learning. It will be very interesting future step for us to look at
39
40 323 both finger and toe PPG traces in our multi-site PPG measurements to see if
41
42 324 classification performance can be boosted significantly.

43
44
45 325 A well-known aspect of PPG measurements is that movement artefact, e.g.
46
47 326 movement of the limb during ambulation or even just whilst a patient is resting
48
49 327 but talking, and changes in body posture can sometimes render a trace unusable
50
51 328 (Carek *et al.*, 2020); Huthart *et al.*, 2020) and so a next step could be to test the
52
53 329 DL-based classifier resilience to certain types of added noise and artefacts. We
54
55
56
57
58
59
60

1
2
3
4 330 would be optimistic that the CNN algorithm, with a max-pooling layer which is
5
6 331 included in AlexNet, could enhance the algorithm robustness to noise, which has
7
8 332 been proven in parallel studies on the DL-based analysis of electrocardiogram
9
10 333 (Muhammed and Aravinth, 2019). The development and application of CNN and
11
12 334 other DL-based methods could be investigated so that reliable evaluation of PAD
13
14 335 can be made in poor quality signals (Waugh *et al.*, 2018).
15
16
17

18 336 *Limitations and further work:* A limitation of our proof-of-concept study is that the
19
20 337 distribution of non-PAD, mild-moderate PAD, and major PAD cases was
21
22 338 unbalanced. A future study should consider assessing unselected patients from
23
24 339 primary care rather than specialist vascular centres. Due to the limitations on
25
26 340 data, we also did not include other (patho-)physiological factors in the model,
27
28 341 such as symptoms, history of heart disease, renal disease, and diabetes, etc. In
29
30 342 future studies, we will recruit a new cohort of cases and controls and include a
31
32 343 comparison with other PAD measures including the Edinburgh Claudication
33
34 344 Questionnaire (ECQ), manual leg pulse palpation, toe systolic pressures, and/or
35
36 345 duplex vascular ultrasound imaging (Kyle *et al.*, 2020). Diabetic patients should
37
38 346 also be studied further particularly the PPG 'AC' and 'DC' lower frequency
39
40 347 components for with and without PAD cases (Bentham *et al.*, 2018). Other CNN
41
42 348 architectures such as LeNet, GoogLeNet, and ResNet can also be tested to see
43
44 349 if they can boost the efficiency and accuracy of the classifications, particularly in
45
46 350 earlier milder cases of disease. Other pathophysiological parameters (e.g.,
47
48 351 symptoms, anatomic factors, and patient-specific risk factors) can be added to
49
50 352 achieve more accurate classification of PAD cases. Finally, based on the Health
51
52 353 Economic Modelling appraisal of the proposed concept technology, miniaturized
53
54
55
56
57
58
59
60

1
2
3
4 354 DL chips and cloud-based computing can be applied to achieve a use-friendly,
5
6 355 cost-effective, and real-time system to improve healthcare services diagnosis,
7
8 356 management, and treatment of PAD.
9
10

11 357

12 358 **5. Summary**

13
14
15
16 359 We have demonstrated in this proof-of-concept study that, with only limited signal
17
18 360 pre-conditioning, our DL-based PPG method can be configured reliably to detect
19
20 361 PAD (as diagnosed by ABPI) from simple toe PPG measurements in a hospital
21
22 362 vascular department setting. The sensitivity of the technique was higher for more
23
24 363 severe disease (i.e., an ABPI<0.5). Further works are already in progress to help
25
26 364 improve the classification algorithm and its resilience to noise and measurement
27
28 365 artefacts. Ultimately, the trajectory for the project area will be to use *explainable*
29
30 366 *AI* techniques to help understand the complex changes in PPG characteristics
31
32
33
34 367 seen with atherosclerosis and in vascular ageing.
35
36
37
38
39
40
41
42
43
44
45
46
47
48
49
50
51
52
53
54
55
56
57
58
59
60

Figure 1: Example spectrograms comparing time-frequency characteristics over a period of 2.5 minutes for the raw unfiltered PPG signals from the great toe. Clear differences can be seen between these PAD and non-PAD examples, for example in pulse harmonics, variability over time as well as the “AC” to “DC” lower frequency components.

Example toe PPG spectrograms comparing subjects with and without significant lower limb PAD

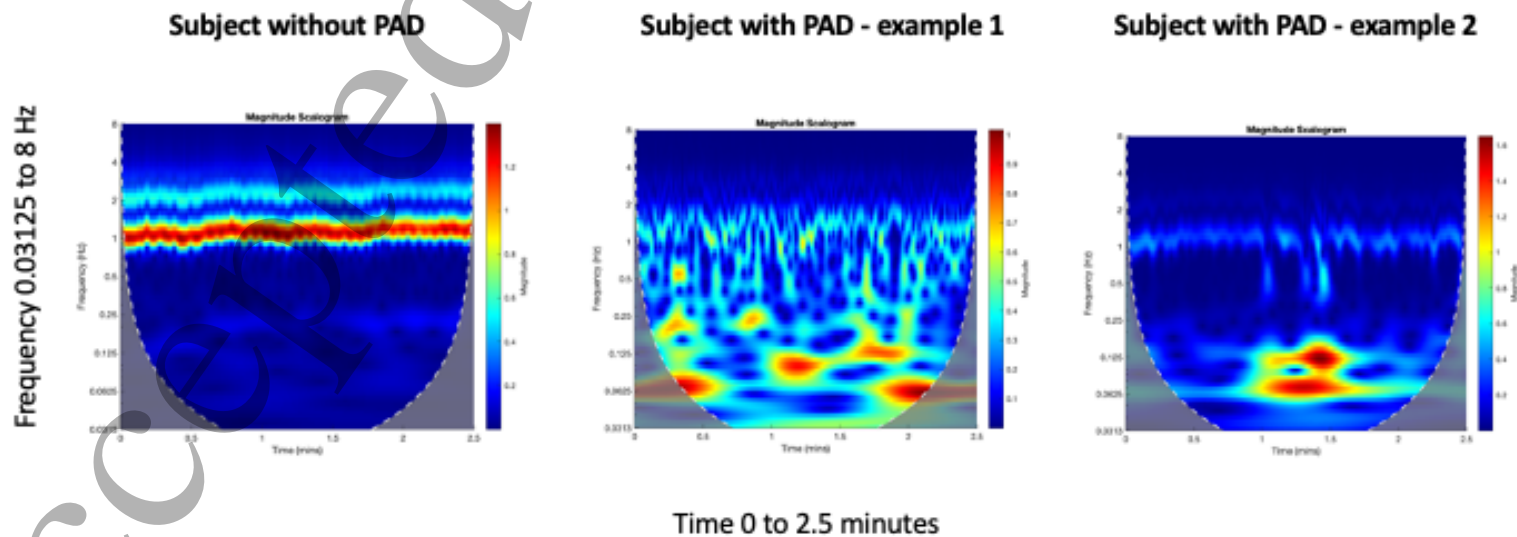
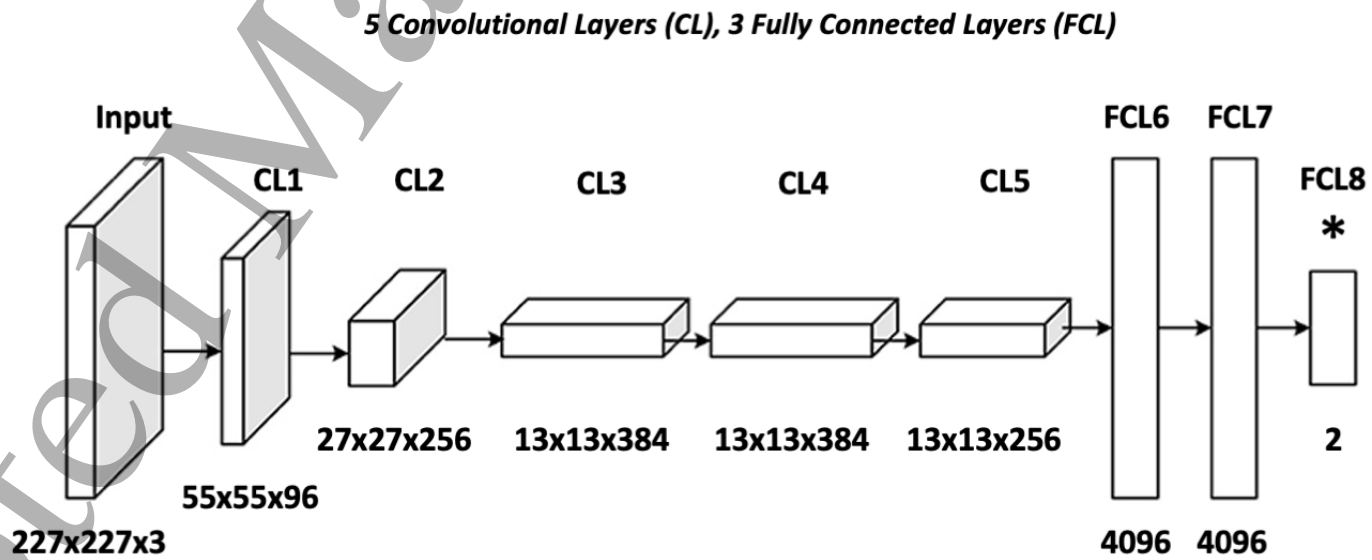


Figure 2: Overview of structure of AlexNet and its tailoring to PPG PAD classification.



*
FCL8 Layer
 23
 24
 25

Original AlexNet
 FCL (1000), pre-trained weights & biases
 Softmax Layer
 Classification Layer
 (= 1000 classes)

Replaced by
 FCL (2 classes), random initialization
 Softmax Layer
 Classification Layer
 (= 2 classes: 'no PAD' and 'PAD')

Tables

Tables 1a and b 5-fold random cross validation with Confusion Matrix from 5 training/validation runs and DTA performance for DLPPG vs ABPI-determined disease (Overall, Mild-Moderate, Major) on a leg basis. Cohen's Kappa statistic for agreement between 2 raters is also give. The 95% Confidence Intervals are shown in brackets.

(a)

Diagnosis by ABPI	DL-based PPG classification	
	No PAD	PAD
No PAD	266	29
Mild-Moderate	23	112
Major	0	37

(b)

	Sensitivity (%)	Specificity (%)	Accuracy (%)	Cohen's Kappa
Overall	86.6 (80.6 – 91.3)		88.9 (85.7 – 91.6)	0.76 (0.70-0.82)
Mild – Moderate	83.0 (75.5 – 88.9)	90.2 (86.2 – 93.3)	87.9 (84.5 – 90.8)	0.72 (0.65-0.79)
Major	100.0 (90.5 - 100.0)		91.3 (87.7 – 94.1)	0.67 (0.56-0.78)

Tables 2a and b 10-fold random cross validation with Confusion Matrix from 10 training/validation runs and DTA performance for DLPPG vs ABPI-determined disease (Overall, Mild-Moderate, Major) on a leg basis. Cohen's Kappa statistic for agreement between 2 raters is also give. The 95% Confidence Intervals are shown in brackets.

(a)

Diagnosis by ABPI	DL-based PPG classification	
	No PAD	PAD
No PAD	258	32
Mild-Moderate	22	75
Major	1	33

(b)

	Sensitivity (%)	Specificity (%)	Accuracy (%)	Cohen's Kappa
Overall	82.4 (74.8 – 88.5)		86.9 (83.3 – 90.0)	0.70 (0.63-0.77)
Mild –	77.3	89.0	86.1	0.64
Moderate	(67.7 – 85.2)	(84.8 - 92.3)	(82.2 – 89.3)	(0.55-0.73)
Major	97.1 (84.7 – 99.9)		89.8 (86.0 – 92.9)	0.61 (0.50-0.73)

References

- 1
2
3
4
5
6
7
8
9
10
11
12
13
14
15
16
17
18
19
20
21
22
23
24
25
26
27
28
29
30
31
32
33
34
35
36
37
38
39
40
41
42
43
44
45
46
47
48
49
50
51
52
53
54
55
56
57
58
59
60
- Abdulhannan P, Russell D A and Homer-Vanniasinkam S 2012 Peripheral arterial disease: a literature review *British Medical Bulletin* **104** 21-39
- Allen J 2002 Measurement and analysis of multi-site photoplethysmographic pulse waveforms in health and arterial disease. Newcastle University, PhD thesis.
- Allen J 2007 Photoplethysmography and its application in clinical physiological measurement *Physiological Measurement* **28** R1-R39
- Allen J and Hedley S 2019 Simple photoplethysmography pulse encoding technique for communicating the detection of peripheral arterial disease—a proof of concept study *Physiological Measurement* **40** 08NT1
- Allen J and Murray A 1993 Development of a neural network screening aid for diagnosing lower limb peripheral vascular disease from photoelectric plethysmography pulse waveforms *Physiological Measurement* **14** 13-22
- Allen J, Oates C P, Lees T A and Murray A 2005 Photoplethysmography detection of lower limb peripheral arterial occlusive disease: a comparison of pulse timing, amplitude and shape characteristics *Physiological Measurement* **26** 811-21
- Allen J, Overbeck K, Nath A F, Murray A and Stansby G 2008 A prospective comparison of bilateral photoplethysmography versus the ankle-brachial pressure index for detecting and quantifying lower limb peripheral arterial disease *Journal of Vascular Surgery* **47** 794-802
- Bentham M, Stansby G and Allen J 2018 Innovative Multi-Site Photoplethysmography Analysis for Quantifying Pulse Amplitude and Timing Variability Characteristics in Peripheral Arterial Disease **6** 81
- Carek A M, Jung H and Inan O T 2020 A Reflective Photoplethysmogram Array and Channel Selection Algorithm for Weighing Scale Based Blood Pressure Measurement *IEEE Sensors Journal* **20** 3849-58
- Chan G, Cooper R, Hosanee M, Welykholowa K, Kyriacou P A, Zheng D, Allen J, Abbott D, Lovell N H, Fletcher R and Elgendi M 2019 Multi-Site Photoplethysmography Technology for Blood Pressure Assessment: Challenges and Recommendations **8** 1827
- Cheng P, Chen Z, Li Q, Gong Q, Zhu J and Liang Y 2020 Atrial Fibrillation Identification With PPG Signals Using a Combination of Time-Frequency Analysis and Deep Learning *IEEE Access* **8** 172692-706
- Dall'Olio L, Curti N, Remondini D, Safi Harb Y, Asselbergs F W, Castellani G and Uh H-W 2020 Prediction of vascular aging based on smartphone acquired PPG signals *Scientific Reports* **10** 19756
- Gerhard-Herman M D, Gornik H L, Barrett C, Barshes N R, Corriere M A, Drachman D E, Fleisher L A, Fowkes F G R, Hamburg N M, Kinlay S, Lookstein R, Misra S, Mureebe L, Olin J W, Patel R A G, Regensteiner J G, Schanzer A, Shishehbor M H, Stewart K J, Treat-Jacobson D, Walsh M E, Halperin J L, Levine G N, Al-Khatib S M, Birtcher K K, Bozkurt B, Brindis R G, Cigarroa J E, Curtis L H, Fleisher L A, Gentile F, Gidding S, Hlatky M A, Ikonomidis J, Joglar J, Pressler S J and Wijeysundera D N 2017 2016 AHA/ACC Guideline on the Management of Patients with Lower Extremity Peripheral Artery Disease: Executive Summary *Vascular Medicine* **22** NP1-NP43
- He R, Huang Z, Ji L, Wu J, Li H and Zhang Z 2016 Beat-to-beat ambulatory blood pressure estimation based on random forest. In: *2016 IEEE 13th International Conference on Wearable and Implantable Body Sensor Networks (BSN)*, pp 194-8

- 1
2
3 Herraiz-Adillo Á, Cavero-Redondo I, Álvarez-Bueno C, Pozuelo-Carrascosa D P and
4 Solera-Martínez M 2020 The accuracy of toe brachial index and ankle brachial
5 index in the diagnosis of lower limb peripheral arterial disease: A systematic
6 review and meta-analysis *Atherosclerosis* **315** 81-92
- 7
8 Huthart S, Elgendi M, Zheng D, Stansby G, Allen J. Advancing PPG signal quality and
9 know-how through knowledge translation- from experts to student. *Frontiers in*
10 *Digital Health – Health Informatics* section. 2020.
11 <https://doi.org/10.3389/fdgth.2020.619692>
- 12 Johnson A E W, et al. 2016 MIMIC-III, a freely accessible critical care database.
13 *Scientific Data* **3** 160035.
- 14 Karimian N, Tehranipoor M and Forte D 2017 Non-fiducial PPG-based authentication
15 for healthcare application. In: *2017 IEEE EMBS International Conference on*
16 *Biomedical & Health Informatics (BHI)*, pp 429-32
- 17 Krizhevsky A, Sutskever I, Hinton GE 2012 Imagenet classification with deep
18 convolutional neural networks. *Advances in neural information processing*
19 *systems* **25** 1097-1105
- 20
21 Kyle D, Boylan L, Wilson L, Haining S, Oates S, Sims A, Guri I, Allen J, Wilkes S,
22 Stansby G 2020 Accuracy of Peripheral Arterial Disease Registers in UK
23 General Practice: Case-Control Study *Angiology*
24 <https://doi.org/10.1177/2150132720946148>
- 25
26 Lee J J, Heo J H, Han J H, Kim B R, Gwon H Y and Yoon Y R 2020 Prediction of
27 Ankle Brachial Index with Photoplethysmography Using Convolutional Long
28 Short Term Memory *Journal of Medical and Biological Engineering* **40** 282-91
- 29 Liang Y, Chen Z, Ward R and Elgendi M 2018 Photoplethysmography and Deep
30 Learning: Enhancing Hypertension Risk Stratification **8** 101
- 31
32 Lu S, Lu Z & Zhang Y D 2019 Pathological brain detection based on AlexNet and transfer
33 learning. *J Computational Science* **30** 41-47
- 34 McHugh M L J B m B m 2012 Interrater reliability: the kappa statistic **22** 276-82
- 35 Muhammed M A A and Aravinth J 2019 CNN based Off-the-Person ECG Biometrics.
36 In: *2019 International Conference on Wireless Communications Signal*
37 *Processing and Networking (WiSPNET)*, pp 217-21
- 38
39 Panwar M, Gautam A, Dutt R and Acharyya A 2020 CardioNet: Deep Learning
40 Framework for Prediction of CVD Risk Factors. In: *2020 IEEE International*
41 *Symposium on Circuits and Systems (ISCAS)*, pp 1-5
- 42 Perpetuini D, Chiarelli A M, Maddiona L, Rinella S, Bianco F, Bucciarelli V, Gallina S,
43 Perciavalle V, Vinciguerra V, Merla A and Fallica G 2019 Multi-Site
44 Photoplethysmographic and Electrocardiographic System for Arterial Stiffness
45 and Cardiovascular Status Assessment **19** 5570
- 46
47 Reiss A, Indlekofer I, Schmidt P and Van Laerhoven K 2019 Deep PPG: Large-Scale
48 Heart Rate Estimation with Convolutional Neural Networks **19** 3079
- 49 Scott J, Lecouturier J, Rousseau N, Stansby G, Sims A, Wilson L and Allen J 2019
50 Nurses' and patients' experiences and preferences of the ankle-brachial pressure
51 index and multi-site photoplethysmography for the diagnosis of peripheral
52 arterial disease: A qualitative study *PLOS ONE* **14** e0224546
- 53
54 Vriens B, D'Abate F, Ozdemir B A, Fenner C, Maynard W, Budge J, Carradice D and
55 Hinchliffe R J 2018 Clinical examination and non-invasive screening tests in the
56 diagnosis of peripheral artery disease in people with diabetes-related foot
57 ulceration *Diabetic Medicine* **35** 895-902
- 58
59
60

- 1
2
3 Wang S-H, Xie S, Chen X, Guttery DS, Tang C, Sun J and Zhang Y-D 2019
4 Alcoholism identification based on an AlexNet transfer learning model *Front.*
5 *Psychiatry* **10** 205. doi: 10.3389/fpsy.2019.00205
6
7 Waugh W, Allen J, Wightman J, Sims A J and Beale T A W 2018 Novel Signal Noise
8 Reduction Method through Cluster Analysis, Applied to Photoplethysmography
9 *Computational and Mathematical Methods in Medicine* 6812404
10
11 Wilkes S, Stansby G, Sims A, Haining S, Allen J 2015 Peripheral arterial disease:
12 diagnostic challenges and how photoplethysmography may help. *British Journal of*
13 *General Practice* **65 (635)**: 323-324 doi.org/10.3399/bjgp15X685489
14
15
16
17
18
19
20
21
22
23
24
25
26
27
28
29
30
31
32
33
34
35
36
37
38
39
40
41
42
43
44
45
46
47
48
49
50
51
52
53
54
55
56
57
58
59
60